

<https://doi.org/10.1038/s41529-024-00514-1>

Dynamic assessment of titanium surface oxides following mechanical damage reveals only partial passivation under inflammatory conditions



Georgios A. Kotsakis¹ ✉, Li Xie^{1,2}, Danyal A. Siddiqui¹, Diane Daubert³, Daniel J. Graham⁴ & Francisco Javier Gil⁵

Motivated by clinical problems of titanium implant degradation, we developed a workflow that enabled assessment of surface oxide dynamics as a function of clinical interventions and inflammation conditions. We found that mechanical damage led to decrease of stoichiometric TiO₂ ratio in the passivation oxide film and further resulted in accelerated degradation under inflammatory anaerobic conditions. This method can be employed for the assessment of surface oxides to monitor implant safety.

Biomaterial degradation *in vivo* has emerged as an important area of implantable biomaterials research. Implantable biomaterials are highly successful in the fields of orthopedic, oral, and maxillofacial rehabilitation. Among these biomaterials, titanium devices are widely used with annual estimates exceeding 1000 tons of titanium being implanted in humans worldwide¹.

Titanium and its alloys are popular as implantable biomaterials thanks to the thin titanium surface oxide “passivation” layer that forms spontaneously and rapidly under atmospheric conditions. This stable, adherent, and tenacious passivation layer prevents corrosion under normal physiological conditions during implantation, thus making titanium implants suitable for long-term functional rehabilitation². Commercially available implantable titanium devices are primarily composed of titanium dioxide (>90%) on the surface layer, with co-existing suboxides (e.g., Ti₂O₃ and TiO) at very small concentrations³. Nonetheless, no metal can completely resist corrosion. Tribocorrosion research has revealed that titanium implants may wear under constant friction^{4–6}. Resulting wear- and dissolution-related degradation products, primarily in the form of titanium particles, are then generated. These implant-derived titanium particles have destructive inflammatory effects leading to clinical morbidity, implant failure, and major health expenditures⁶. However, titanium biomaterial improvements have been impeded by the lack of suitable tools and workflows to assess titanium surface oxide dynamics in relevant biological systems. Existing analytical tools, such as X-ray photoelectron spectroscopy (XPS)

composition analysis, are limited to assessment of direct wear effects because robust temporal assessments in biological fluids are impeded by organic surface contamination⁷. The absorption of organic contaminants obstructs elemental composition analysis and impedance measurements. This is particularly relevant in oral implant research because the transgingival nature of these implants results in their coverage by polymicrobial biofilms and their extracellular matrix within hours of their implantation⁸. These surface layers make it difficult to determine the effects of surface contamination and surface treatment interventions on the composition and fine structure of titanium oxides. These layers must be removed before one can probe the titanium surface. For instance, in a recent study of UV light treatment for removal of titanium surface saliva contaminants, the restoration of titanium atomic percentages increased by 10-fold following 15 min of UV light irradiation⁹. However, the lack of chemical state analysis from high-resolution spectra prohibited the study of whether the intervention led to changes in surface oxide composition or partial surface titanium restoration with unstable oxides, which may have accounted for comparable numbers of necrotic osteoblastic cells on the UV-treated surfaces versus saliva contaminated surfaces⁹. Additionally, it has been recognized that once the integrity of the passivation film is destroyed, if it cannot be repaired immediately, titanium will no longer be immune to corrosion and could be vulnerable in corrosive environments¹⁰. Specifically, titanium particles resulting from implant corrosion and degradation have been linked to severe cytotoxicity and pro-inflammatory cellular responses^{11,12}.

¹Rutgers School of Dental Medicine, Newark, NJ, USA. ²State Key Laboratory of Oral Diseases, National Clinical Research Center for Oral Diseases, West China Hospital of Stomatology, Sichuan University, Chengdu, Sichuan, China. ³School of Dentistry, University of Washington, Seattle, WA, USA. ⁴Department of Bioengineering, University of Washington, Seattle, WA, USA. ⁵Bioengineering Institute of Technology, Universitat Internacional de Catalunya (UIC), Sant Cugat del Vallés, Barcelona, Spain. ✉e-mail: gk567@sdm.rutgers.edu

Monitoring titanium bonding states should provide information on the mode of recovery of biomaterial surfaces after functional wear challenges in orthopedic implants and after surface biofilm removal interventions in oral implants. High-resolution XPS (HR-XPS) spectral analysis enables collection of specific data of individual element oxidation states. Therefore, HR-XPS has recently emerged as a powerful approach for the identification of different surface oxides by indirectly assessing metal atom bonding states¹³. Additionally, argon sputtering prior to XPS analyses could provide effective removal of surface contaminants¹³. For instance, a recent study of failed and retrieved dental implants employed HR-XPS to show that areas of surface alterations and discolorations in failed implants were consistent with altered oxidation states of titanium, such as Ti_2O_3 and even a metallic Ti peak¹⁴. Further, a study comparing hip and knee Ti and CoCrMo alloys leveraged HR-XPS to detect critical differences in the surface chemistry of different titanium alloys retrieved from failed implants with adequate sensitivity to discriminate between different compositions of titanium alloys¹⁵. Nonetheless, a comprehensive longitudinal assessment of the spatial and temporal variations in surface passivation states following routine decontamination treatments, and its subsequent impact on titanium dissolution, has not yet been conducted.

Here, we address this gap by presenting a comprehensive workflow for an optimized approach that assesses changes in titanium surface oxides and resulting metal dissolution rates.

A brief introduction of the study

As shown in Fig. 1, we first simulated clinical conditions by obtaining microrough Ti surfaces and culturing a polymicrobial biofilm derived from peri-implant human plaque¹⁶. Information on the growth of the multi-species clinical biofilm is provided in the supplemental information as previously described¹⁶. Biofilm samples retained multiple oral taxa, with an enrichment of gram-negative taxa known to be prevalent in peri-implantitis,

such as *S. sanguinis*, *V. parvula*, and *Neisseria* species¹¹. Subsequently, the samples were treated by different clinical decontamination treatments to simulate dental implant cleaning interventions that are common in practice¹⁷. We selected two means of chemical surface treatment (acidic citric acid (CA) or alkaline sodium hypochlorite (NaOCl)), and two mechanical means of surface treatment (abrasive titanium brush (Ti-brush) or non-abrasive nylon (Ny) brush). The SEM images of the surface with biofilm and after Ti-brush treatment are shown in Supplementary Fig. 1. A monoatomic argon beam was used to sputter the titanium substrate to remove organic contaminants until titanium signal could be observed and HR-XPS was conducted for characterization of chemical bonding states of Ti element. Supplementary Fig. 2 showed a typical XPS depth profile after argon beam sputtering. It can be observed that the peak intensity of carbon elements remarkably reduced after argon beam sputtering. Finally, ICP-MS was used to detect titanium dissolution after aging in artificial saliva to mimic inflammation conditions for 31 days in an anaerobic environment as previously described¹⁸.

HR-XPS detection after clinical intervention

As shown in Fig. 2, high-resolution Ti 2p XPS spectra indicated different composition of titanium oxides among these groups. Specifically, it was observed that use of the Ti brush significantly lowered the $\text{TiO}_2\%$ (~66.7%) as compared to all other non-abrasive groups (~90%). In addition, the percentage of Ti% (6.6%) in Ti-brush group was remarkably higher than those in other groups (1.8–2.1%). The remarkable decrease of the percentage of TiO_2 and increase of Ti indicated a damage of the surface passivation layer since previous studies revealed that the topmost layer of the naturally formed titanium passivation film is composed of over 90% of TiO_2 ^{13,19}. Further detection with XPS small spot analysis provided a more direct verification of surface changes. The optical images taken in the XPS vacuum chamber showed two distinct areas in the Ti-brush-treated samples as seen

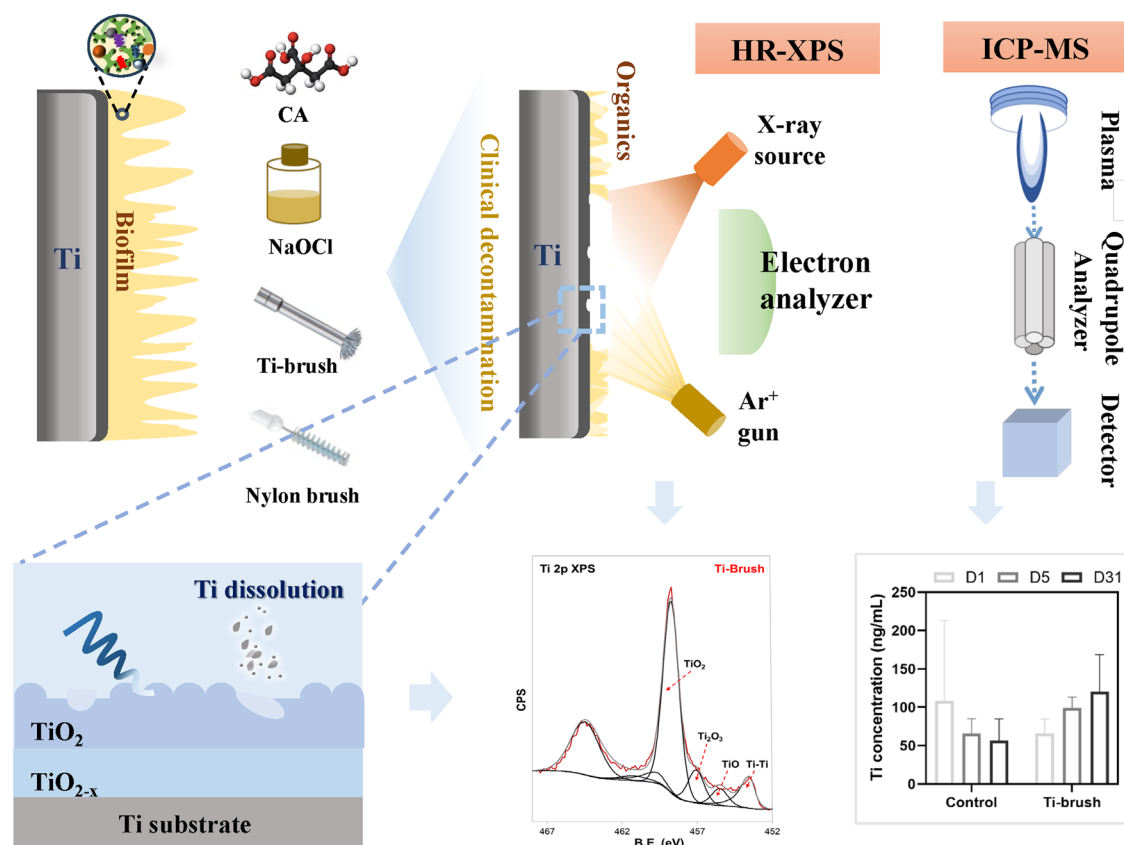


Fig. 1 | Experimental Workflow. Schematic illustration of multilevel titanium passivation layer assessment performed after argon beam surface contaminant removal, focused XPS surveys for spatially informed analyses, and metal dissolution analyses by ICP-MS.

Fig. 2 | High Resolution XPS Elemental Analysis. A Stack plots of the high-resolution Ti 2p peaks from each of the samples after different treatments. A representative peak fitting is shown for the Ti-Brush sample at the bottom of the figure. For all samples, the binding energy has been referenced to the TiO₂ peak at 459.1 eV. B Table and (C) Histogram images of chemical composition of different titanium oxides calculated by peak fitting of the high-resolution Ti 2p data.

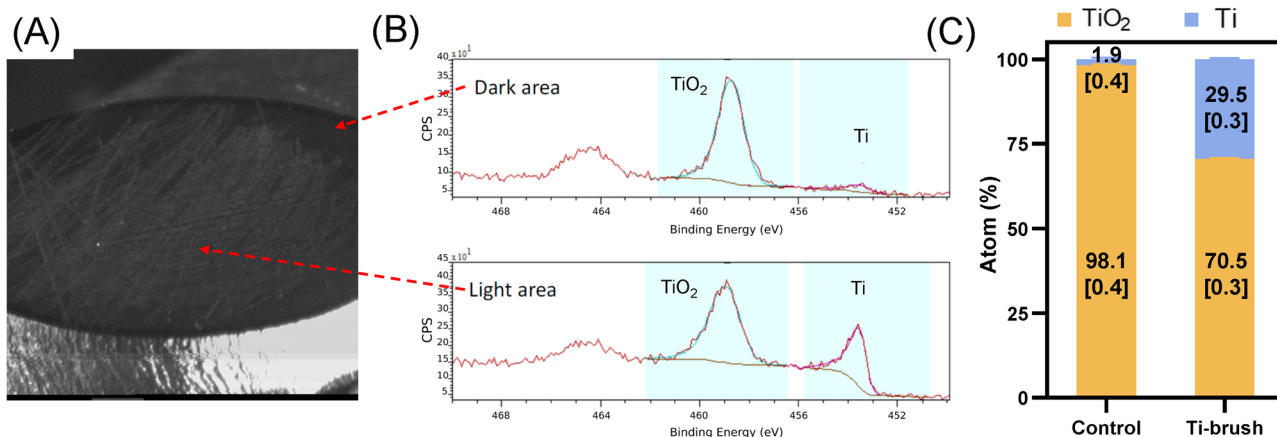
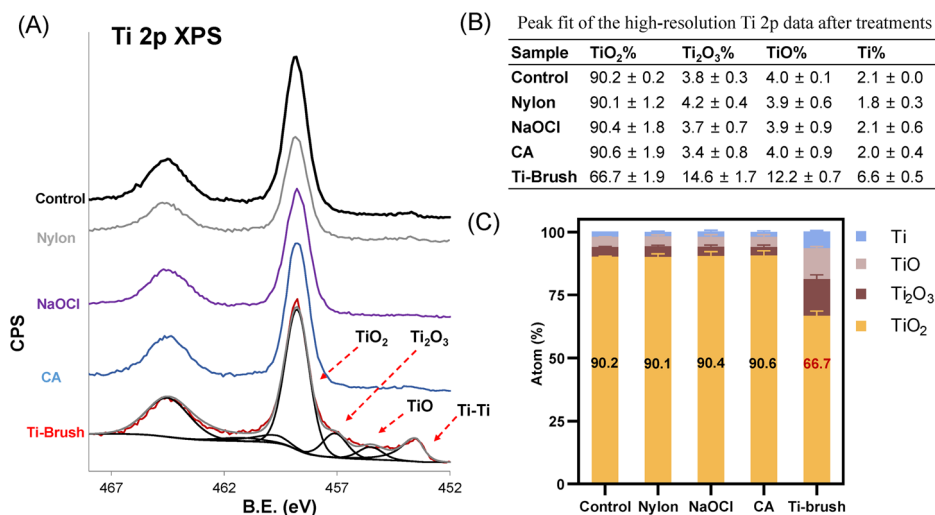


Fig. 3 | Spatially focused High Resolution XPS. A Camera view of the scraped sample shows visual differences indicating the Ti-brush curretted area could possibly be identified visually. Light areas appear to be the curretted region and dark areas

appear to be un-curretted. B The corresponding XPS Ti 2p spectra of the dark area and light area. C The Histogram image of the chemical composition of TiO₂ and Ti calculated from the high-resolution Ti 2p data.

in Fig. 3. The light grey streaks (light area, Fig. 3A) represent areas abraded by the Ti brush (i.e., “scratched”), where there was a damage in the oxide layer (TiO₂:70.5), while the dark areas represent Ti surface not touched by the Ti brush, which retained a very high (98.1%) coverage by TiO₂. This data difference suggests that the topmost passivation layer had been abraded and damaged by the Ti-brush abrasion. Overall, the above data demonstrated that the Ti-brush treatment caused damage to the original passivation film, while other treatments (including CA, NaOCl, and Nylon) did not.

HR-XPS and ICP-MS detection after aging

Next, we analyzed whether the damaged oxide film could be repassivated in biological conditions by aging for 31 days in simulated inflammatory conditions using a previously established electrolytic solution rich in proteins under anaerobic conditions¹¹. These conditions simulate the inflammatory environmental conditions in peri-implantitis disease. In addition, an assay was devised to assess if the changes in passivation layer would further affect titanium dissolution from the surface¹⁸.

The HR-XPS data revealed that for the Ti-brush treated group after 31 days of aging in artificial saliva, the XPS Ti 2p spectrum generally matched with the unaged control sample, and the percentage of TiO₂ was also similar with the unaged control sample (See Figs. 2 and 4). This indicated that the passivation layer failed to recover¹³. As further shown by the calculated composition data from the curve fitting spectra (Fig. 4B), the relative percentage of the TiO₂ (66.6%) for the Ti-brush group was the lowest among

the groups, whereas the percentage of the Ti metal state (13.3%) was the highest. As shown in Supplementary Table 1 and Supplementary Fig. 3, the ratio of Ti increased compared to samples before aging across all samples. This trend was consistently observed following the aging process. However, they still showed higher values (69.6–88%) compared with that of Ti-brush sample (66.6%). Furthermore, it appears that all samples underwent a reduction process (Ti(IV) to Ti(III); Ti(II) to Ti(0)) during aging, as indicated by the ratio change trends of titanium valence states. In addition, all groups, except the Ti-brush group, showed a reduction in TiO₂ composition percentages after aging, suggesting possible passivation film damage during aging.

It is commonly recognized that titanium will spontaneously and quickly re-passivate after being damaged due the high affinity between titanium and oxygen under aerobic conditions¹⁹. However, the passivation behavior of titanium alloys is affected by many factors, such as the corrosive environment in which they are exposed with oxygen availability being the most decisive factor^{4,18}. Importantly, in our experiments, the inflammation-mimic aging condition which recapitulated the anaerobic conditions in the peri-implant sulcus environment in human disease was found to hinder the re-passivation of the film and even will accelerate its degradation⁴. This finding in our study is consistent with a previous study carried out by Sridhar et al., which showed that oxide layer of titanium dental implants became thinner in late-stage implant retrievals (implant loose due to severe peri-implantitis) demonstrated by HR-XPS detection²⁰. Because the

Fig. 4 | Effects of Ageing on Passivation Layer Composition. **A** An overlay of the Ti 2p peak of Ti-brush sample before and after exposure to the artificial saliva. **B** Histogram images of chemical composition of different titanium oxides calculated by peak fitting of high-resolution Ti 2p data analyzed after artificial saliva immersion. Control represents the unaged control abraded samples.

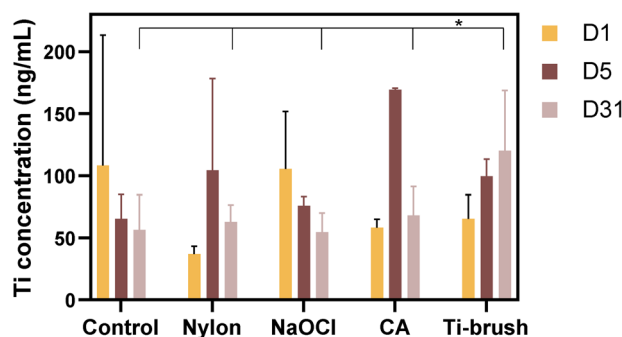
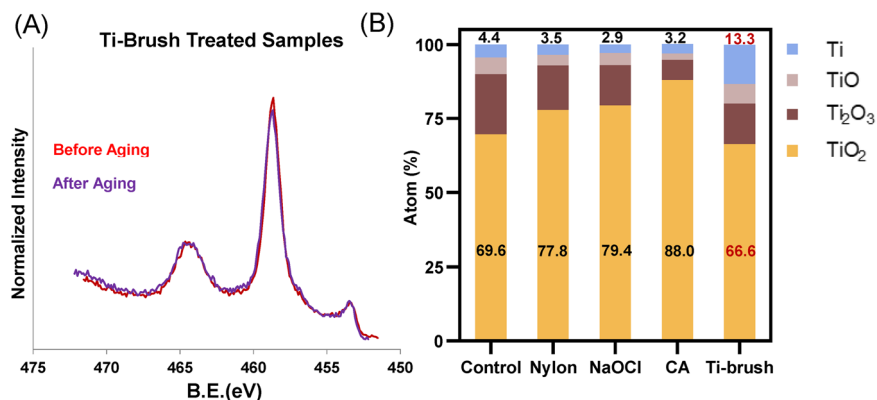


Fig. 5 | Titanium release over time. Analyzed by ANOVA with post-hoc tests at $\alpha = 0.05$. (* $p < 0.05$).

titanium oxide film requires an oxygen environment for forming or recovering. Therefore, the oxygen-depleted environment in peri-implant sulcus makes it difficult for damaged oxide film to repassivate completely¹⁸. Koike and Fujii proved that titanium is more prone to corrosion when oxygen shortage is present in environment²¹.

Additionally, the ICP-MS data (Fig. 5) show that the concentration of the dissolved Ti for the Ti-brush-treated samples increased with time, while other groups did not display the same trend. On day 31, the Ti-brush group exhibited the largest value of Ti ions concentration, nearly 2-fold higher compared with the control as well as the other groups ($p < 0.05$). These data indicated that the incomplete passivation film could accelerate titanium corrosion and release of titanium ions or microparticles. Wang et al. reported that the TiO₂/Ti₂O₃ ratio of the passivation film was directly related to the polarization and anti-corrosion performance of the titanium substrates¹³. It is also well known to all that the stoichiometric TiO₂ is the most chemically stable form compared with other titanium oxides with lower valence states²². The decreased proportions of TiO₂ in the other aging groups also revealed a partially damaged or impaired topmost passivation layer when subjected to the inflammation-mimic conditions. Of note, although it is recognized that the argon sputtering could damage the oxides during bombardment²³, the data in this study still solidly demonstrate the significant difference between the Ti brush treatment and other treatments since the same sputtering parameters were used for all samples both for the direct assessments and the aging experiments.

In this work, we presented a complete workflow of an optimized approach to assess temporal changes of titanium oxide composition and resulting metal dissolution rates. These findings highlight the detrimental effects of certain mechanical treatments on the fine composition and chemical state of the passivation film of dental implants. This general method can be employed for the spatiotemporal assessment of titanium or other metal alloy surface oxides to improve biomedical implant safety²⁴.

Summarizing, we used monoatomic argon sputtering to remove bio-film contaminants to expose the titanium surface and then carried out HR-XPS and small spot XPS to determine composition changes of titanium oxide passivation films after various decontamination methods. It was found that the Ti-brush treatment would probably damage the topmost TiO₂ layer and greatly reduce the TiO₂ ratio in the passivation layer. It was also found that this compromised passivation film did not recover after aging in simulated inflammatory conditions under anaerobic aging. As a result, accelerated titanium corrosion occurred in the Ti-brush group. The proposed detection approaches have promise as a valuable tool for the identification of chemical composition and valence state of the metal passivation films. Additionally, these findings raise future concerns regarding safety evaluations for empirical decontamination and the need for innovation in effective repassivation strategies.

Methods

Titanium samples

Ti grade V (Ti-6Al-4V) disks with a diameter of 10 mm were acid etched following a proprietary etching protocol to obtain microrough surfaces identical to commercial dental implants¹¹. Prior to experiments, surface contaminants were removed by ultrasonication in cyclohexane followed by washing in acetone and ethanol and deionized (DI) water. Disks were sterilized via autoclaving for 15 min at 121 °C. Depending on the assays, sterile acid-etched Ti disks, or identical Ti disks with the peri-implantitis biofilm model were treated with clinically relevant mechanical treatments and/or chemotherapeutic agents (Fig. 1).

Biofilm culture

To test our hypotheses while ascertaining a high translational potential we used a clinically relevant peri-implantitis model, which employs multi-species human plaque biofilms, as previously described¹⁶. The biofilm was grown anaerobically (Anaerobic glove box, 37 °C, N₂, and H₂ 95:5 [vol/vol]) on 10 mm diameter titanium disks for 48 h. For between-experiment reproducibility in the biofilm assays the approximate number of bacteria in liquid culture was standardized via OD600 and incubation times were optimized in pilot time series experiments to consistently yield high-coverage robust biofilms with > 95% viability.

Surface decontamination

The simulated clinical treatments were selected based on commonly utilized interventions by practitioners for implant hygiene. Two means of chemical surface treatment (acidic citric acid (CA) or alkaline NaOCl), and two mechanical means of surface treatment (abrasive titanium brush (Ti-brush) or non-abrasive nylon (Ny) brush) were selected as representatives. When 0.9% Sterile saline solution (Control) was utilized as negative control, respectively, titanium disks were immersed in it for 30 s. For mechanical treatments, all interventions were applied for 30 s on the titanium surfaces utilizing a surgical implant motor function at 300 RPMs (Nylon (Ny) brush

and Titanium (Ti) brush, Salvin Item# ROTOBRUSH-DELTA-S). Titanium disks were immersed in 20% citric acid or 5% NaOCl for 30 s, respectively.

- (A) Control group (Ctrl): sterilized acid-etched Ti surface.
- (B) Nylon brush group (Ny): Ctrl + 30 s mechanical treatment with a nylon brush.
- (C) Ti brush group (Ti-brush): Ctrl + 30 s mechanical treatment with a titanium brush, the information of titanium brush used: Salvin Roto-Brush-Titanium® Thread Cleaning Brush For Wide Area-Short.
- (D) Citric acid group (CA): Ctrl + 30 s immersion in 20% citric acid.
- (E) NaOCl group: Ctrl + 30 s immersion in 5% NaOCl.

Aging in simulated saliva

We assessed whether titanium surface passivation layer damage by mechanical interventions leads to increased titanium dissolution by assessing titanium dissolution after 1, 5, and 31 days of material aging of treated samples according to our previous literature¹¹. To eliminate wear particle effects and focus on long-term titanium dissolution products only, we eliminated any titanium particles generated as direct effects of the mechanical interventions by repeated rinsing with phosphate-buffered saline PBS for three times and transfer to fresh glass vials to avoid titanium particle entrapment in plastic. Samples ($n = 3$ for each group) were immersed in a protein-rich electrolyte solution simulating tissue fluids (Minimum Essential Medium (MEM) & 10% Fetal bovine serum (FBS)) in anaerobic conditions (Anaerobic glove box, 37 °C, N₂, and H₂ (95:5 [vol/vol])) for 1, 5, and 31 days.

X-ray photoelectron spectroscopy (XPS)

All sample handling was done with double solvent-cleaned tools; the solvents were HPLC-grade acetone and methanol. All XPS spectra were taken on a Kratos Axis Ultra photoelectron spectrometer²⁵. This instrument has a monochromatized Al K α X-ray and a low-energy electron flood gun for charge neutralization of non-conducting samples. X-ray analysis was taken in Kratos “slot” mode. The area for these acquisitions was approximately 300 × 700 μm . Pressure in the analytical chamber during spectral acquisition was less than 5×10^{-9} torr. The take-off angle (the angle between the sample normal and the input axis of the energy analyzer) was 0°, (0° take-off angle corresponds with an approximate sampling depth of 100 Å). Before analysis, a monoatomic argon sputter source was used to sputter each sample until titanium signal was detected and the oxygen signal reached a maximum or plateaued. Sputtering was done over a 1000 μm × 1000 μm area. Spectra were collected within the center of the sputtered area. Survey spectra from three different spots were collected on each sample. Detailed scans of Sn (tin) and N (nitrogen) were taken to better quantify small amounts of these elements. The pass energy for survey and detail spectra (to calculate composition) was 160 eV. The pass energy for high-resolution Ti 2p spectra was 20 eV.

For small spot analysis of the scraped sample, visibly different areas were identified using the optical camera view of the Kratos instrument. A 100 μm spot was centered in a scraped and un-scraped area to assure that signal was only coming from the selected area. High-resolution scans of the Ti 2p peak were taken to distinguish between metallic titanium and oxidized titanium.

All data was analyzed using CasaXPS analysis software to calculate the elemental compositions from peak areas²⁵. A Shirley background was used for calculating composition information and for peak fitting. High-resolution Ti 2p peaks were fit using Gaussian peaks with 30% Lorentzian character. All components were fit using two peaks for the Ti 2p_{3/2} and Ti 2p_{1/2} spin-orbit split peaks with a 2:1 area ratio. The parallel sample number for each group in clinical intervention treatment experiments was three. The sample number was one for each group in aging experiments.

Inductively coupled mass spectrometry (ICP-MS)

Degraded titanium concentrations were determined at endpoint via Inductively Coupled Mass Spectrometry (ICP-MS) as previously described²⁶. They

were transferred to digestion vessels (50 mL polypropylene centrifuge tubes) with four 1-mL rinses of digestion solution (50:50 V/V) concentrated nitric acid trace-metal grade: deionized (DI) water with a trace amount of hydrofluoric acid and 10 ppm terbium as recovery standard. Each sample was brought to 5 mL with the digestion solution. Open vessel microwave digestion was used (power 800 W, 100%, ramp 15 min to 100 °C, hold for 45 min). After the digestion, samples were brought to 25 mL with DI water. Analysis for titanium was conducted by ICP-MS with a detection limit of 0.5 ng. The parallel sample number for each group in aged ICP-MS experiments was three. Data were analyzed by ANOVA with post-hoc tests at $\alpha = 0.05$.

Data availability

The authors declare that all data supporting the findings of this study will be made available upon request.

Received: 8 July 2024; Accepted: 10 September 2024;

Published online: 17 September 2024

References

- Jung, H. D. Titanium and its alloys for biomedical applications. *Met. Basel* **11**, 1945 (2021).
- Sittig, C., Textor, M., Spencer, N. D., Wieland, M. & Vallotton, P. H. Surface characterization of implant materials cp Ti, Ti-6Al-7Nb and Ti-6Al-4V with different pretreatments. *J. Mater. Sci. Mater. M* **10**, 35–46 (1999).
- Wheelis, S. E., Wilson, T. G., Valderrama, P. & Rodrigues, D. C. Surface characterization of titanium implant healing abutments before and after placement. *Clin. Implant Dent. R.* **20**, 180–190 (2018).
- Apaza-Bedoya, K. et al. Synergistic interactions between corrosion and wear at titanium-based dental implant connections: a scoping review. *J. Periodontol Res* **52**, 946–954 (2017).
- Wu, H. et al. A wear-resistant TiO nanoceramic coating on titanium implants for visible-light photocatalytic removal of organic residues. *Acta Biomater.* **97**, 597–607 (2019).
- Chen, L. et al. Titanium particles in peri-implantitis: distribution, pathogenesis and prospects. *Int J. Oral. Sci.* **15**, 49 (2023).
- Yang, T. et al. Residual extracellular polymeric substances (EPS) detected by fluorescence microscopy on dental implants after different decontamination. *Mater. Chem. Phys.* **296**, 127242 (2023).
- Veerachamy, S., Yarlagaadda, T., Manivasagam, G. & Yarlagaadda, P. K. D. V. Bacterial adherence and biofilm formation on medical implants: a review. *P I Mech. Eng. H.* **228**, 1083–1099 (2014).
- Hirota, M. et al. Impaired osteoblastic behavior and function on saliva-contaminated titanium and its restoration by UV treatment. *Mat. Sci. Eng. C. Mater.* **100**, 165–177 (2019).
- Yang, X. J., Du, C. W., Wan, H. X., Liu, Z. Y. & Li, X. G. Influence of sulfides on the passivation behavior of titanium alloy TA2 in simulated seawater environments. *Appl Surf. Sci.* **458**, 198–209 (2018).
- Kotsakis, G. A. et al. Effect of implant cleaning on titanium particle dissolution and cytocompatibility. *J. Periodontol.* **92**, 580–591 (2021).
- Eger, M. et al. Mechanism and prevention of titanium particle-induced inflammation and osteolysis. *Front Immunol.* **9**, 2963 (2018).
- Wang, L. et al. Local fine structural insight into mechanism of electrochemical passivation of titanium. *Acs Appl Mater. Inter* **8**, 18608–18619 (2016).
- Sridhar, S. et al. Multifaceted roles of environmental factors toward dental implant performance: Observations from clinical retrievals and testing. *Dent. Mater.* **34**, E265–E279 (2018).
- Jenko, M. et al. Surface chemistry and microstructure of metallic biomaterials for hip and knee endoprostheses. *Appl Surf. Sci.* **427**, 584–593 (2018).
- Lamont, E. I. et al. Modified SHI medium supports growth of a disease-state subgingival polymicrobial community in vitro. *Mol. Oral. Microbiol* **36**, 37–49 (2021).

17. Monje, A. et al. Strategies for implant surface decontamination in peri-implantitis therapy. *Int J. Oral. Impl.* **15**, 213–249 (2022).
18. Berbel, L. O., Banczek, E. D. P., Karoussis, I. K., Kotsakis, G. A. & Costa, I. Determinants of corrosion resistance of Ti-6Al-4V alloy dental implants in an In Vitro model of peri-implant inflammation. *PLoS One* **14**, e0210530 (2019).
19. Cao, H. L. & Liu, X. Y. Activating titanium oxide coatings for orthopedic implants. *Surf. Coat. Tech.* **233**, 57–64 (2013).
20. Sridhar, S. et al. Multifaceted roles of environmental factors toward dental implant performance: observations from clinical retrievals and in vitro testing. *Dent. Mater.* **34**, e265–e279 (2018).
21. Koike, M. & Fujii, H. The corrosion resistance of pure titanium in organic acids. *Biomaterials* **22**, 2931–2936 (2001).
22. Podshivalova, A. K. & Karpov, I. K. Thermodynamic analysis of the stability of titanium oxides in the TiO–TiO range. *Russ. J. Inorg. Chem.* **52**, 1147–1150 (2007).
23. Greczynski, G. & Hultman, L. Towards reliable X-ray photoelectron spectroscopy: Sputter-damage effects in transition metal borides, carbides, nitrides, and oxides. *Appl Surf. Sci.* **542**, 148599 (2021).
24. Vasconcelos, D. M., Santos, S. G., Lamghari, M. & Barbosa, M. A. The two faces of metal ions: from implants rejection to tissue repair/regeneration. *Biomaterials* **84**, 262–275 (2016).
25. Biesinger, M. C., Lau, L. W. M., Gerson, A. R. & Smart, R. S. C. Resolving surface chemical states in XPS analysis of first row transition metals, oxides and hydroxides: Sc, Ti, V, Cu and Zn. *Appl Surf. Sci.* **257**, 887–898 (2010).
26. Safioti, L. M., Kotsakis, G. A., Pozhitkov, A. E., Chung, W. O. & Daubert, D. M. Increased levels of dissolved titanium are associated with peri-implantitis—a cross-sectional study. *J. Periodontol.* **88**, 436–442 (2017).

Acknowledgements

This study was supported by the UW RRF (Kotsakis, G, PI) and by NIDCR R03DE029872 and R01DE031746 (Kotsakis G, PI). Part of this work was conducted at the Molecular Analysis Facility, a National Nanotechnology Coordinated Infrastructure (NNCI) site at the University of Washington, which is supported in part by funds from the National Science Foundation (awards NNCI-2025489, NNCI-1542101), the Molecular Engineering & Sciences Institute, and the Clean Energy Institute.

Author contributions

G.A.K. conceptualized the work. G.A.K. and L.X. prepared the draft and figures and revised the paper. D.A.S. and D.J.G. participated in the data collection and paper revision. D.J.G. conducted XPS measurements. D.D., F.J.G. participated in the paper revision. All authors have read and agreed to the published version of the manuscript.

Competing interests

The authors declare no competing interests.

Additional information

Supplementary information The online version contains supplementary material available at <https://doi.org/10.1038/s41529-024-00514-1>.

Correspondence and requests for materials should be addressed to Georgios A. Kotsakis.

Reprints and permissions information is available at <http://www.nature.com/reprints>

Publisher's note Springer Nature remains neutral with regard to jurisdictional claims in published maps and institutional affiliations.

Open Access This article is licensed under a Creative Commons Attribution-NonCommercial-NoDerivatives 4.0 International License, which permits any non-commercial use, sharing, distribution and reproduction in any medium or format, as long as you give appropriate credit to the original author(s) and the source, provide a link to the Creative Commons licence, and indicate if you modified the licensed material. You do not have permission under this licence to share adapted material derived from this article or parts of it. The images or other third party material in this article are included in the article's Creative Commons licence, unless indicated otherwise in a credit line to the material. If material is not included in the article's Creative Commons licence and your intended use is not permitted by statutory regulation or exceeds the permitted use, you will need to obtain permission directly from the copyright holder. To view a copy of this licence, visit <http://creativecommons.org/licenses/by-nc-nd/4.0/>.

© The Author(s) 2024